of Ni(tetraene)$^{2+}$ (–0.26 V vs NHE) is in the range where electron-transfer quenching would be expected to occur, and thus the larger quenching rate suggests that most of the quenching by this complex occurs via electron transfer. However, transient absorption measurements failed to reveal the existence of either the Ni^{II}(tetraene)$^{+}$ radical or $Ru(bpy)_3^{3+}$ after the quenching event, indicating that if electron-transfer quenching does occur, most of the products undergo back electron transfer in the initial solvent cage.

The unimolecular energy-transfer rate constant for the bpy-cyclamNi^{2+} pendant complex can be estimated from the bimolecular quenching data. The rate constant for the bimolecular quenching, k_q, of $Ru(bpy)_3^{2+}$ by Ni(cyclam)$^{2+}$ is 1.5×10^8 M^{-1} s^{-1} at 20 °C. Moreover, $k_q = K_{eq}k_e$, where K_{eq} is the equilibrium constant for the formation of the reactant precursor complex [e.g., $Ru(bpy)_3^{2+}|NiL^{2+}$] and k_e is the first-order rate constant for energy transfer within this complex. The equilibrium constant can be estimated from Debye–Huckel expressions[37] as ~0.5 M^{-1}. This gives $k_e \sim 3 \times 10^8$ s^{-1} at room temperature; the rate constant for energy transfer within the pendant complex would be expected to have a similar value. Thus, in the bpy-cyclamNi^{2+} pendant complex the energy-transfer pathway could play an important role in determining the rate of excited-state decay. However, the lifetime of the complex is also expected to be affected by the rate of deactivation of the ^{3}MLCT state via the ^{3}LF state of Ru. This rate constant can be estimated from the lifetime of the bpy-cyclamH_2^{2+} pendant complex and is thus expected to be about 2×10^8 s^{-1} at room temperature, a value similar to the energy-transfer rate constant estimated above. Thus, for the bpy-cyclamNi^{2+} pendant complex near room temperature, deactivation both by a strong-coupling nonradiative decay to a ruthenium-centered ligand-field state and by energy transfer to a nickel-centered ligand-field state may contribute to the rate of deactivation of the ^{3}MLCT state. This suggestion is supported by the difference in k_0 and k_1 for the bpy-cyclamH_2^{2+} and bpy-cyclamNi^{2+} pendant complexes. At all temperatures studied, the observed rates for the slow and fast components of the decay of the bpy-cyclamNi^{2+} pendant complexes in EtOH are faster than the corresponding rates of the bpy-cyclamH_2^{2+} pendant complex. This is also true for the calculated value of k_1 at room temperature. Likewise, k_0 is larger for the nickel complex, while the energy gap ($\Delta G°$) between the emissive ^{3}MLCT state and the ground state for the two complexes is similar. Thus the energy-transfer pathway may contribute to the low-temperature rate.[38]

(37) Sutin, N.; Brunschwig, B. S. *ACS Symp. Ser.* **1982**, *No. 198*, 105.

Conclusions

1. For $Ru(bpy)_2bpy-L^{2+}$ complexes substituted at the 6 position of the bipyridine ring, steric hindrance by the 6-methyl group or the 6-methylene bridge causes an increase in the Ru–N bond distance, a decrease of the ligand-field strength, and a lowering of the energy of the excited ligand-field states and/or changes in their metal–ligand distortion (λ) relative to the ^{3}MLCT and ground states. These changes dramatically decrease the lifetimes of the ^{3}MLCT excited state of these complexes near room temperature due to an increase in the temperature-dependent deactivation rate via a strongly-coupled ligand-field state.

2. For the $Ru(bpy)_2$(bpy-cyclamNi)$^{4+}$ complex, two channels may contribute to the excited-state decay at room temperature. Deactivation takes place via strong coupling to a ruthenium-centered ligand-field excited state and possibly via energy transfer to a nickel-centered ligand-field state. Thus the observed quenching of the ^{3}MLCT state is due entirely to enhancement of the nonradiative decay channels.

3. The enhancement of the ligand-field decay channels in these 6-substituted Ru(bpy) complexes is an undesirable complication in catalytic systems. When a mediator or catalyst is attached to a photosensitizer, the substitution should not either lower the energy of any of the sensitizers's deactivating excited states or introduce low-energy excited states on the mediator which quench the sensitizer. Either case will reduce the yield of the desired electron-transfer quenching pathway and decrease catalytic activity.

Acknowledgment. We thank Drs. Carol Creutz and Norman Sutin for helpful discussions, Dr. Siegfried Schindler for synthetic suggestions, and Elinor Norton for analyses for ruthenium, nickel, PF_6^-, and ClO_4^- and measurements of mass spectra. This research was carried out at Brookhaven National Laboratory under Contract DE-AC02-76CH00016 with the U.S. Department of Energy and supported by its Division of Chemical Sciences, Office of Basic Energy Sciences.

(38) It would be expected that this pathway would have a temperature-dependent rate. However, extraction of another set of activation parameters from the data is not possible.

Contribution from the Arthur Amos Noyes Laboratory,† California Institute of Technology, Pasadena, California 91125, and Department of Chemistry, University of Pittsburgh, Pittsburgh, Pennsylvania 15260

Fluorescence Excitation Spectra of Quadruply Bonded $M_2X_4L_4$ Complexes

Vincent M. Miskowski,*,‡ Harry B. Gray,*,‡ and Michael D. Hopkins*,§

Received August 19, 1991

Fluorescence excitation spectra have been obtained by monitoring the emissive $^1(\delta\delta^*)$ excited states of $Mo_2X_4(PMe_3)_4$ (X = Cl, Br, I), $Mo_2Cl_4(AsMe_3)_4$, and $W_2Cl_4(PMe_3)_4$ in solution at 300 and 77 K. The polarization ratios of these transitions, and their shifts in energy arising from substitution of the metal and ligand, have been correlated with predictions derived from available theoretical calculations and photoelectron spectroscopic data to yield self-consistent assignments of all observed bands in the UV region. These bands, with the exception of a poorly characterized one at the edge of the vacuum-UV region, are assigned to singlet excitations from metal–metal (δ, σ, π) and ligand (σ(MP), σ(MX), π(X)) orbitals to the δ^* orbital.

Complexes of the $M_2X_4L_4$ class (M = Mo, W; X = Cl, Br, I; L = P or As donor) have proven to be valuable subjects of research into the nature and properties of the metal–metal quadruple bond, in large part because the wide range of systematic electronic perturbations that can be achieved through ligand and metal substitution allows elucidation of metal–metal and metal–ligand properties.[1,2] Although most of the attention devoted to these compounds has focused on the δ and δ^* orbitals and the electronic

† Contribution No. 8499.
‡ California Institute of Technology.
§ University of Pittsburgh.

(1) (a) Hopkins, M. D.; Miskowski, V. M.; Gray, H. B. *J. Am. Chem. Soc.* **1988**, *110*, 1787–1793. (b) Hopkins, M. D.; Schaefer, W. P.; Bronikowski, M. J.; Woodruff, W. H.; Miskowski, V. M.; Dallinger, R. F.; Gray, H. B. *J. Am. Chem. Soc.* **1987**, *109*, 408–416. (c) Hopkins, M. D.; Zietlow, T. C.; Miskowski, V. M.; Gray, H. B. *J. Am. Chem. Soc.* **1985**, *107*, 510–512. (d) Zietlow, T. C.; Hopkins, M. D.; Gray, H. B. *J. Solid State Chem.* **1985**, *57*, 112–119. (e) Hopkins, M. D.; Gray, H. B. *J. Am. Chem. Soc.* **1984**, *106*, 2468–2469. (f) Hopkins, M. D. Ph.D. Thesis, California Institute of Technology, 1986.

0020-1669/92/1331-2085$03.00/0

transitions between them, we recently reported[1a] the results of single-crystal polarized electronic absorption measurements of visible and near-ultraviolet bands attributable to $^3(\sigma \rightarrow \delta^*)$, $^1(\pi \rightarrow \delta^*)$, and $^{1,3}(\sigma(MP) \rightarrow \delta^*)$ transitions.

In this report, we present the fluorescence excitation spectra of $Mo_2X_4L_4$ (X = Cl, Br, I; L = PMe_3, $AsMe_3$) and $W_2Cl_4(PMe_3)_4$. Determination of the fluorescence polarization ratios permits assignment of the polarization of the electronic absorption bands that lie in the UV region, all of which were much too intense to be measured in our earlier single-crystal polarized absorption study.[1a] These intense bands are of interest for the following reasons: first, because at least some of the metal–metal-localized electronic transitions involving the strongly bonding metal–metal orbitals (e.g., $\pi \rightarrow \pi^*$, $\sigma \rightarrow \sigma^*$) should appear in this region or at still shorter wavelength; second, because ligand-to-metal charge-transfer (LMCT) transitions of photochemical interest[3] fall in the UV region; and third, because coupling with LMCT transitions has been proposed[4] to be the source of most of the observed intensity of the $^1(\delta \rightarrow \delta^*)$ transition.

Experimental Section

The compounds $Mo_2Cl_4(PMe_3)_4$,[5a] $Mo_2Br_4(PMe_3)_4$,[1b] $Mo_2I_4(PMe_3)_4$,[1b] $Mo_2Cl_4(AsMe_3)_4$,[1b] and $W_2Cl_4(PMe_3)_4$[5b] were prepared according to standard procedures. Solutions of slightly air-sensitive $W_2Cl_4(PMe_3)_4$ were prepared in an argon-filled glovebox; those of the other compounds proved to be sufficiently air stable that such treatment was unnecessary.

Fluorescence and fluorescence excitation spectra were recorded on a Perkin-Elmer MPF-66 emission spectrometer. Excitation spectra were obtained with monitoring at the wavelength of maximum fluorescence intensity. Spectra were corrected using manufacturer-supplied software. Most spectra recorded were for 2-methylpentane (Phillips) solutions; all solutions were optically dilute (o.d. < 0.1/cm). For room-temperature excitation spectra, recorded with the use of 1-cm × 1-cm cuvettes, we attempted to correct for the significant solvent absorption at $\lambda \leq 230$ nm; in the 90° emission geometry of our spectrometer, the solvent/cuvette (1-cm path length) absorbance versus air was divided by 2 for the estimated correction. Measurements in acetonitrile and dichloromethane employed spectroscopic quality solvents (Burdick and Jackson) and were treated similarly.

Measurements at 77 K employed a finger dewar with samples held in sealed quartz EPR tubes. The absorption of the solvent/tube/dewar combination could not be directly measured; we did not attempt to correct for it, but conclude from comparisons to reference absorption spectra[1a] that it is negligible in the $\lambda \geq 240$ nm region.

Polarized fluorescence excitation spectra were acquired using a matched pair of Glan-Taylor air-spaced calcite polarizers held in rotatable mounts in front of the emission and excitation ports of the spectrometer. We additionally mounted, in various experiments, polarization scramblers (Optics for Research) between the spectrometer ports and the polarizers for either or both emission and excitation sides. Corrected (as described below) spectra were insensitive to the use of scramblers for these strongly luminescent compounds. The polarizers absorb strongly for $\lambda \geq 250$ nm; examples of excitation spectra corrected for polarizer absorption of excitation light will be presented later.

Polarized fluorescence excitation spectra at 77 K were acquired for each compound as four data files labeled I_{vv}, I_{vh}, I_{hv}, and I_{hh}, corresponding to the excitation (first index) or emission (second index) transmitting vertical (v) or horizontal (h) polarized light in the 90° emission geometry. The ratio I_{hv}/I_{hh} would theoretically be unity[6] for an ideal spectrometer and sample. We have chosen the simplest of the several equivalent ways[6] of representing emission excitation polarization data, presenting the emission polarization ratio $N = I_{\parallel}/I_{\perp} = (I_{vv}/I_{vh})(I_{hh}/I_{hv})$. ($N$ is, for example, related to the degree of polarization $P = (N - 1)/(N + 1)$.) In the equation for N, the second term in parentheses corrects for nonideal spectrometer effects.[6] We found that I_{hh}/I_{hv}, while not equal to 1, was wavelength independent for all of our measurements. Because of this, it is reasonable to define corrected values of $I_{\parallel} = I_{vv}(I_{hh}/I_{hv})$ and $I_{\perp} = I_{vh}$, and we display several spectra in this form. Finally, we note that the "isotropic equivalent" glass excitation spectrum (that is, a spectrum that would be equivalent to the isotropic absorption spectrum if the emission quantum yield were wavelength independent) is given by $(I_{\parallel} + 2I_{\perp})/3$.[6]

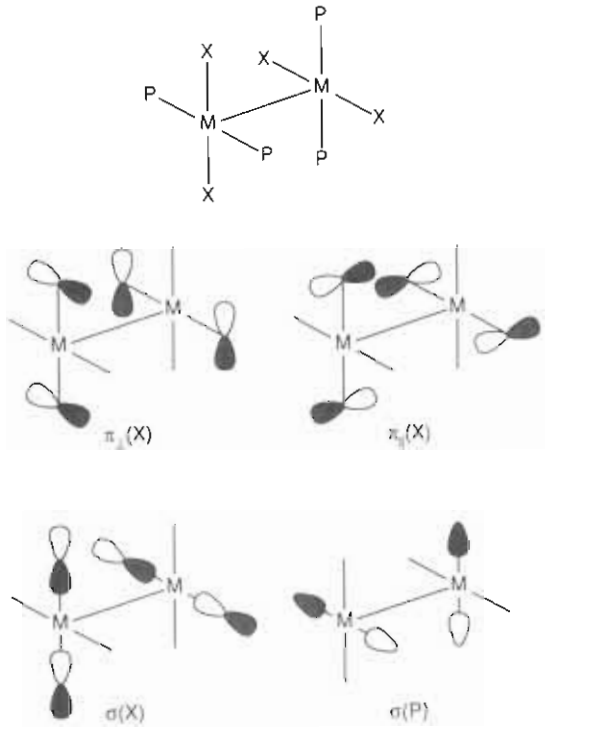

Figure 1. Ligand group orbitals of e symmetry. In each case, only one component is shown.

Results and Discussion

Theory and Photoelectron Spectroscopy. In our previous work,[1] we assigned a number of electronic transitions of the $M_2X_4L_4$ complexes, all of which involved excitations into the $a_2(\delta^*(M_2))$ LUMO. (Hereafter we will drop the M_2 designation for metal–metal orbitals.) The highest energy of these, at 30 860 cm^{-1} for $Mo_2Cl_4(PMe_3)_4$ (band II in our previous labeling),[1a,b] was assigned to the $^1(e(\sigma(MoP)) \rightarrow \delta^*)$ transition.

The photoelectron spectrum of $Mo_2Cl_4(PMe_3)_4$ displays[7] a very intense, broad, ligand-based[7,8] ionization, centered 1.57 eV to higher energy of the $e(\sigma(MoP))$ ionization,[9] as the next feature. This presumably contains the other $\sigma(MoP)$ orbitals and all or most of the $\pi(Cl)$ and $\sigma(MoCl)$ levels, which leads to the prediction that the other $L \rightarrow \delta^*$ transitions of $Mo_2Cl_4(PMe_3)_4$ should be centered around 43 500 cm^{-1} (about 1.6 eV above the $^1(e(\sigma(MoP)) \rightarrow \delta^*)$ transition).

More detailed predictions can be derived from theoretical calculations on $Mo_2Cl_4(PH_3)_4$.[7,10] The various computational methods employed in these calculations yield widely differing estimates of the atomic-orbital contributions to the molecular orbitals, presumably as a result of the well-known basis-set sensitivity of Mulliken population analysis, although the relative energies of these levels are, on the whole, consistent with the photoelectron data. Specifically, a total of eleven levels of largely $\pi(Cl)$, $\sigma(Cl)$, and $\sigma(P)$ parentage are calculated to lie 1–3 eV

(2) Cotton, F. A.; Walton, R. A. *Multiple Bonds Between Metal Atoms*; Wiley: New York, 1982.
(3) Trogler, W. C.; Gray, H. B. *Nouv. J. Chem.* **1977**, *1*, 475–477.
(4) Hopkins, M. D.; Gray, H. B.; Miskowski, V. M. *Polyhedron* **1987**, *6*, 705–714.
(5) (a) Cotton, F. A.; Extine, M. W.; Felthouse, T. R.; Kolthammer, B. W. S.; Lay, D. G. *J. Am. Chem. Soc.* **1981**, *103*, 4040–4045. (b) Schrock, R. R.; Sturgeoff, L. G.; Sharp, P. R. *Inorg. Chem.* **1983**, *22*, 2801–2806.
(6) Lakowicz, J. R. *Principles of Fluorescence Spectroscopy*; Plenum Press: New York, 1983.
(7) Cotton, F. A.; Hubbard, J. L.; Lichtenberger, D. L.; Shim, I. *J. Am. Chem. Soc.* **1982**, *104*, 679–686.
(8) Root, D. R.; Blevins, C. H.; Lichtenberger, D. L.; Sattelberger, A. P.; Walton, R. A. *J. Am. Chem. Soc.* **1986**, *108*, 953–959.
(9) It has been noted by others[8] that the relative high energy of the $e(\sigma(MP))$ level probably results in part from this level being nonbonding to the (a_1, b_2) pair of $d_{x^2-y^2}$-derived $\sigma^*(ML)$ levels.
(10) (a) Ziegler, T. *J. Am. Chem. Soc.* **1984**, *106*, 5901–5908. Ziegler, T. *J. Am. Chem. Soc.* **1985**, *107*, 4453–4459. We thank Prof. Ziegler for providing us with unpublished details of his calculations (see Figure 1 in ref 1a). (b) Bursten, B. E.; Schneider, W. F. *Inorg. Chem.* **1989**, *28*, 3292–3296. (c) Schneider, W. F.; Bursten, B. E. Private communication of the results of DV-Xα calculations on $Mo_2Cl_4(PH_3)_4$ and $Mo_2Br_4(PH_3)_4$.

Table I. UV Electronic Absorption Data for $M_2X_4L_4$ Complexes in 2-Methylpentane Solution at 300 K[a]

assgnt[b]	band	$Mo_2Cl_4(PMe_3)_4$	$Mo_2Cl_4(AsMe_3)_4$[c]	$Mo_2Br_4(PMe_3)_4$	$Mo_2I_4(PMe_3)_4$	$W_2Cl_4(PMe_3)_4$
$^1(e(\sigma(MP)) \rightarrow \delta^*)$	II	30 860 (3720)	30 960 (3630)	28 990 (6650)	25 320 (11 850)	34 130 (9090)
$^1(b_1(\pi_\perp(X)) \rightarrow \delta^*)$	VII	*d*	*d*	32 200 sh (1200)	29 800 (1880)	38 200 sh (4700)
$^1(e(\pi_\parallel(X)) \rightarrow \delta^*)$	VIII	37 700 sh (2100)	*d*	35 500 sh (3100)	35 000 sh (4400)	42 500 sh (6600)
$^1(e(\pi_\perp(X)) \rightarrow \delta^*)$	IX	42 900 sh (10 400)	41 200 (14 900)	39 500 (8300)	40 000 sh (17 000)	47 600 (19 900)
$^1(e(\sigma(MX)) \rightarrow \delta^*)$	X	47 200 (23 400)	46 000 (23 600)	46 800 sh (21 000)	42 000 (20 400)	>50 000 (>22 000)
$X(np \rightarrow (n+1)s)$; $^1(\pi \rightarrow \pi^*)$; $^1(\sigma \rightarrow \sigma^*)$	XI	*e*	*e*	>50 000 (>30 000)	51 300 (38 000)	*e*

[a] Entries are in the form $\bar{\nu}_{max}/cm^{-1}$ (ϵ_{max}/M^{-1} cm^{-1}); sh = shoulder. [b] See ref 16. [c] For this compound, band II is the analogous σ(MoAs) excitation. See ref 1b. [d] Not resolved at room temperature. [e] Not observed.

below e(σ(MoP)). Among these are four levels that are of the proper symmetry to yield dipole-allowed transitions to δ^*: three e levels (x,y ($\perp z$) polarization) and a b_1 level ($\parallel z$ polarization).

The forms of the zero-order e levels that mix to yield the actual orbitals[7,10] are illustrated in Figure 1. The π(X) orbitals can be divided into two sets: those that are oriented perpendicular to the metal–metal bond ($\pi_\perp$(X): $b_1 + a_2 + e$) and those that are parallel to it ($\pi_\parallel$(X): $a_1 + b_2 + e$). Among these, the b_1 and a_2 $\pi_\perp$(X) orbitals are bonding with respect to δ and δ^*, respectively, and e($\pi_\parallel$(X)) is bonding with respect to both the π and π^* metal–metal levels; in the limit of $\angle MMX = 90°$, the remaining π(X) orbitals are nonbonding. The σ(X) and σ(P) type orbitals each yield a_1, b_2, and e levels, the first two of which are bonding with respect to the metal $d_{x^2-y^2}$ orbitals and the latter of which are nonbonding.

When chloride is replaced by bromide or iodide, we expect the π(X) levels to be destabilized. The first-order effect will be to decrease the energy of σ(MoX) and π(X) $\rightarrow \delta^*$ transitions, but mixing among such states and those derived from σ(MoP) $\rightarrow$ M and metal–metal-localized excitations will also be increased, leading to complications as noted further on. A recent DV–Xα calculation[10c] on $Mo_2Br_4(PH_3)_4$ is consistent with these expectations. A calculation and the photoelectron data for $W_2Cl_4(PMe_3)_4$ indicate a situation closely analogous to that of $Mo_2Cl_4(PMe_3)_4$,[7] but with metal levels destabilized relative to ligand levels; LMCT transitions should thus be blue-shifted.

A second type of excited state that merits consideration involves excitation into virtual orbitals other than δ^*. There is no experimental work available that gives the location of such levels for these compounds, but recent DV–Xα calculations[10c] place σ^* and π^*, respectively, ca. 1.6 and 2.3 eV to higher energy of δ^* for $Mo_2Cl_4(PH_3)_4$. No electronic transitions to π^* or σ^* could be conclusively identified in our previous work.[1a] The lowest-energy transitions to these levels, namely, interconfigurational excitations of the type $\delta \rightarrow \pi^*$, $\pi \rightarrow \sigma^*$, etc., are expected to be very weak features like the previously identified[1a] $\pi \rightarrow \delta^*$ and $\sigma \rightarrow \delta^*$ bands and, if they occur in the UV region (as is suggested by the calculations[10c]), are therefore likely to be obscured by strong charge-transfer absorptions. Among the intraconfigurational excitations, which will yield $\parallel z$-polarized absorptions, the $^1(\pi \rightarrow \pi^*)$ transition is expected to yield an intense band, because it is strongly metal–metal bonding-to-antibonding. While the intensity of the $^1(\sigma \rightarrow \sigma^*)$ band would be predicted to be comparable to that of $^1(\pi \rightarrow \pi^*)$ on the basis of a simple metal d-orbital model, it may, in fact, be relatively modest, given the moderate bonding and antibonding character, respectively, attributed to the highest-energy σ level and the lowest-energy σ^* level by theoretical calculations and the results of photoelectron experiments.[8,10]

We finally consider spin-forbidden excitations. The $^3(e(\sigma(MP)) \rightarrow \delta^*)$ transition has been experimentally located[1a] as a weak feature 5000 cm^{-1} below the corresponding singlet excitation. Ab initio calculations by Hay[11] on $Re_2Cl_8^{2-}$ indicate that excited-state singlet–triplet splittings of the same magnitude are reasonable in most cases. Prominent exceptions are bonding–antibonding transitions: the $\delta \rightarrow \delta^*$ excitation, for which, as previously discussed by us in detail,[1c,4] the singlet and triplet excited states are strongly split by virtue of the fact that, in valence-bond terms, the former is ionic in character while the latter is covalent; and the $\pi \rightarrow \pi^*$ and $\sigma \rightarrow \sigma^*$ excitations, which are expected to share these peculiarities. Hay's calculation supports this: the singlet and triplet $\pi \rightarrow \pi^*$ excited states—there are totals of four of each—are predicted to be spread out over 30 000 cm^{-1}.

Electronic Absorption Spectra. Table I summarizes the room-temperature UV absorption spectra of the $M_2X_4L_4$ compounds. Figures showing these spectra have been presented in a previous paper.[1b] The only band in this region whose assignment has been previously considered is band II,[1a,b] which was identified as $^1(e(\sigma(MP)) \rightarrow \delta^*)$. To higher energy of this band, between two and five intense bands, plus a number of weaker features, are observed. We have numbered these as bands VII–XI, extending the labeling scheme of our previous work.[1a] Absorption spectra have also been measured for glassy solutions of several of these compounds at 77 K. These are in general agreement with the fluorescence excitation spectra to be presented below.

It is worth noting that the solvent dependence of the visible and UV absorption bands is negligible for all compounds. Thus, absorption maxima in the solvents 2-methylpentane and acetonitrile agree to within 500 cm^{-1} for all compounds.

Room-Temperature Emission Excitation Spectra. In an early paper,[12] it was noted that the $^1(\delta^* \rightarrow \delta)$ fluorescence quantum yield of the compound $Mo_2Cl_4(PBu^n_3)_4$ in hydrocarbon solution is independent of excitation wavelength in the range 250–600 nm. In our present work we have established that fluorescence excitation spectra for the compounds $Mo_2Cl_4(PMe_3)_4$ and $Mo_2Cl_4(AsMe_3)_4$ in hydrocarbon solution precisely match absorption spectra for excitation wavelengths as short as 220 nm. Thus, the emission quantum yield is wavelength independent over the entire accessible absorption spectrum, which indicates that all of the corresponding excited states internally convert to the emissive $^1(\delta\delta^*)$ state with near-unit efficiency. Among other things, this implies that unimolecular photoreactions, such as halogen-radical release, cannot be significant processes for any of these excited states.

For $Mo_2Br_4(PMe_3)_4$ we observe a modest difference between excitation and absorption spectra (Figure 2). After correction of the excitation spectrum for solvent absorption, it is still less intense than the absorption spectrum in the $\lambda < 225$-nm region. There is a more significant difference between excitation and absorption spectra of $Mo_2I_4(PMe_3)_4$ for $\lambda < 260$ nm, as shown in Figure 3. For this compound, it appears that the excited state produced by the intense absorption feature that maximizes at 195 nm is not funneling its excitation into the $^1(\delta\delta^*)$ excited state with unit efficiency; there is a ~50% loss at 200 nm. We suggest that the smaller effects seen for $Mo_2Br_4(PMe_3)_4$ may reflect an analogous excited state whose corresponding absorption maximum lies at $\lambda < 200$ nm.[13]

We have also measured excitation spectra in acetonitrile and dichloromethane and find similar agreements of absorption and excitation spectra up to near the solvent absorption limit. In

(11) Hay, P. J. *J. Am. Chem. Soc.* **1982**, *104*, 7007–7017.

(12) Miskowski, V. M.; Goldbeck, R. A.; Kliger, D. S.; Gray, H. B. *Inorg. Chem.* **1979**, *18*, 86–89.

(13) We have not directly looked for photochemistry emanating from this high-energy state, because we lack suitable deep-UV excitation sources. However, we note that no photodecomposition was observed during our measurements. This suggests that the nonemissive internal-conversion channel for this state in hydrocarbon solvent is simply direct nonradiative decay to the ground state, bypassing the emissive $^1(\delta\delta^*)$ state.

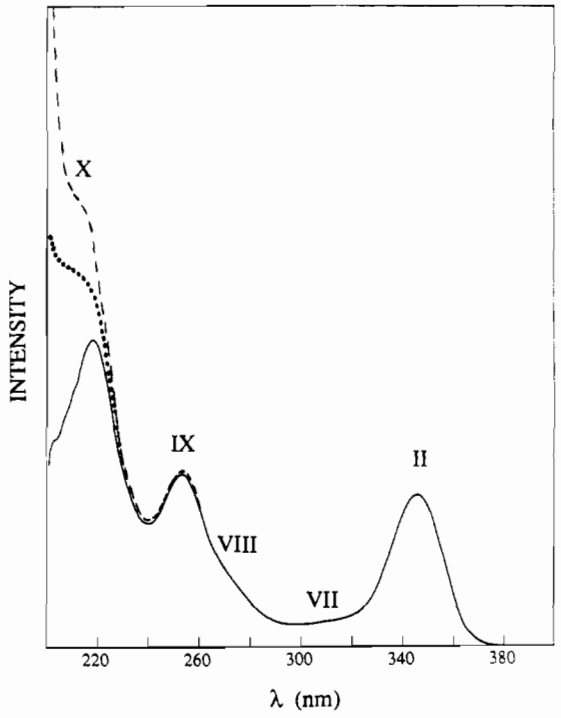

Figure 2. Absorption spectrum (---) and fluorescence excitation spectra of $Mo_2Br_4(PMe_3)_4$ in 2-methylpentane at 300 K: (—) excitation spectrum, uncorrected for solvent absorption; (···) excitation spectrum, corrected for solvent absorption. Spectra are scaled to the 345-nm band.

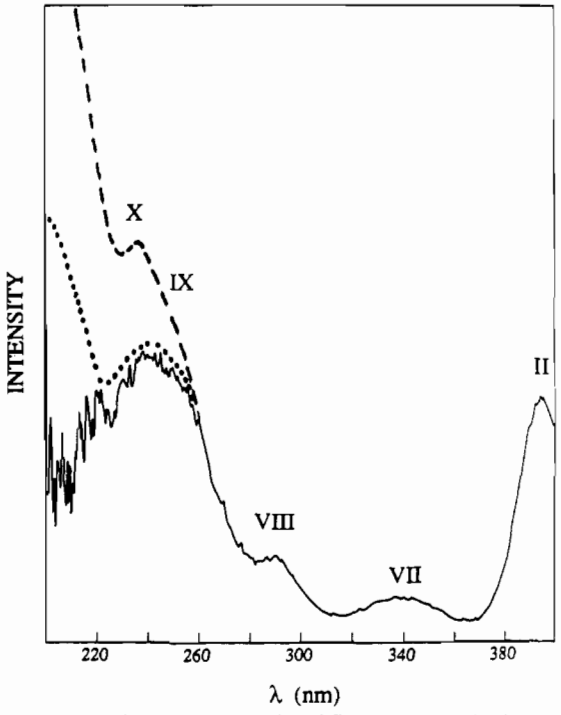

Figure 3. Absorption spectrum (---) and fluorescence excitation spectra of $Mo_2I_4(PMe_3)_4$ in 2-methylpentane at 300 K: (—) excitation spectrum, uncorrected for solvent absorption; (···) excitation spectrum, corrected for solvent absorption. Spectra are scaled to the 396-nm band.

acetonitrile, for which we can extend the measurement down to 200 nm, there is again a significant deviation between fluorescence excitation profile and electronic absorption spectrum for $Mo_2I_4(PMe_3)_4$.

Low-Temperature Polarized Fluorescence Excitation Spectra. Polarized fluorescence excitation spectra (Figures 4–8) were measured for the $M_2X_4L_4$ compounds in 2-methylpentane at 77 K. Our results are summarized in Table II. From single-crystal polarized spectra, we have previously established[1f] the fluorescence

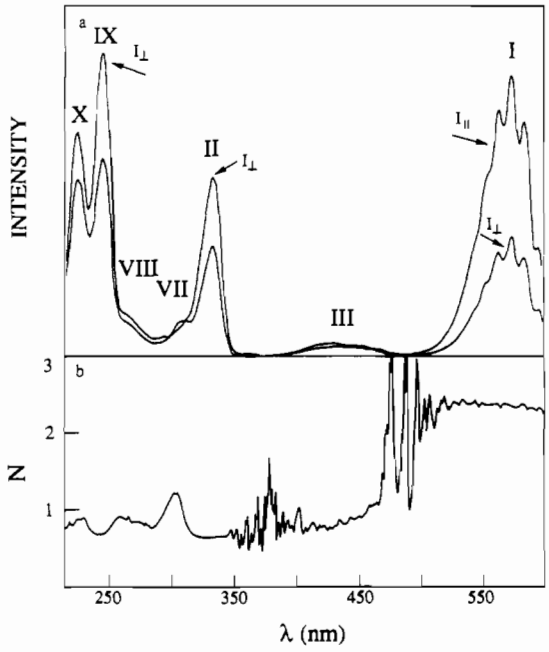

Figure 4. (a) Polarized fluorescence excitation spectra of $Mo_2Cl_4(AsMe_3)_4$ in 2-methylpentane at 77 K. (b) Wavelength dependence of N for (a).

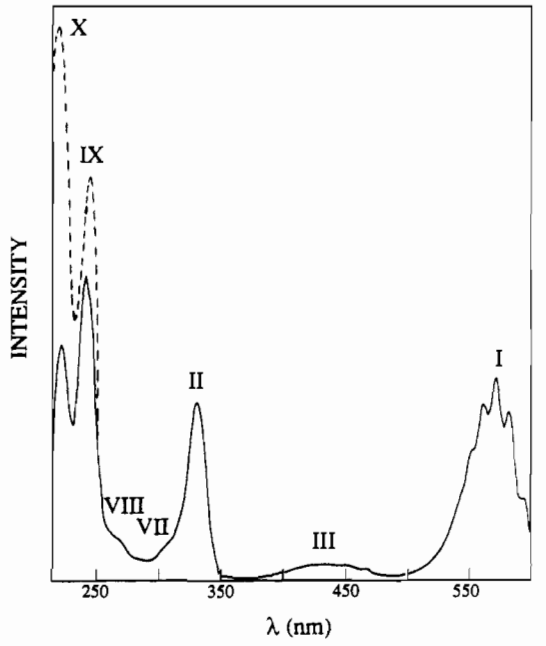

Figure 5. Isotropic-equivalent fluorescence excitation spectra ($I_\parallel + 2I_\perp$) of $Mo_2Cl_4(AsMe_3)_4$ in 2-methylpentane at 77 K: (—) uncorrected for polarizer absorption; (---) corrected for polarizer absorption.

to be $\parallel z$-polarized and have also determined[1a] the polarizations of bands I–III. For a D_{2d}-symmetry molecule held in a rigid matrix, dipole-allowed electronic absorption bands coupled to $\parallel z$-polarized emission can result in either of two theoretical values[6] of the polarization ratio: $N = 3$ if the absorption band is allowed $\parallel z$ or $N = 0.5$ if the absorption band is allowed with $\perp z$ polarization. Instrumentation factors aside, experimental values of N are always degraded somewhat toward depolarization ($N = 1$) by sample imperfections (strain, scattering at boundaries, etc.).[6] For our apparatus and for several well-established test molecules, the experimental values of N corresponding to the theoretical values of 3 and 0.5 prove to be 1.9–2.4 and 0.6–0.7, respectively.

Our results for bands I–III (Table II) are consistent with theory. Band I ($N = 2.0$–2.4) has been established to be the very strongly $\parallel z$-polarized $^1(\delta \rightarrow \delta^*)$ transition, while band II ($N = 0.6$–0.65) is the equally strongly $\perp z$-polarized $^1(e(\sigma(MP)) \rightarrow \delta^*)$ transition.

Table II. Fluorescence Excitation Data for $M_2X_4L_4$ Complexes in 2-Methylpentane at 77 K[a]

assgnt[b]	band	$Mo_2Cl_4(PMe_3)_4$	$Mo_2Cl_4(AsMe_3)_4$[c]	$Mo_2Br_4(PMe_3)_4$	$Mo_2I_4(PMe_3)_4$	$W_2Cl_4(PMe_3)_4$
$^1(\delta \rightarrow \delta^*)$	I	17 120 (2.2)	17 420 (2.4)	16 780 (2.2)	15 770 (2.2)	15 270 (2.0)
$^1(e(\sigma(MP)) \rightarrow \delta^*)$	II	30 120 (0.65)	30 030 (0.6)	28 570 (0.6)	25 450 (0.6)	33 840 (0.6)
$^1(\pi \rightarrow \delta^*)$	III	22 730 (0.9)	23 640 (0.8)	22 080 (0.8)	20 750 (0.8)	20 410 (0.7)
$^3(e(\sigma(MP)) \rightarrow \delta^*)$	IV	*d*	*d*	*d*	*d*	27 250 sh (0.65) 29 675
$^1(b_1(\pi_\perp(X)) \rightarrow \delta^*)$	VII	33 560 (1.4)	32 470 (1.2)	31 950 (1.7)	29 400 (1.9) 30 600 sh (1.4)	37 175 (0.65) 38 500 sh
$^1(e(\pi_\parallel(X)) \rightarrow \delta^*)$	VIII	37 040 sh (0.8) 38 910 sh (0.9)	36 100 sh (0.8) 37 700 sh (0.9)	35 970 sh (0.7) 37 040 (0.9)	33 000 sh (1.2) 34 600 (0.7) 37 300 sh (0.8)	42 550 sh (1.0)
$^1(e(\pi_\perp(X) \rightarrow \delta^*)$	IX	42 920 sh (0.8)	41 150 sh (0.6)	39 680 (0.9)	39 400 (0.7)	~45 000[e,f] (~1.5)
$^1(e(\sigma(MX)) \rightarrow \delta^*)$	X	44 840[e] (1.0)	44 840[e] (0.8)	42 370 (0.8)	41 850 (1.3)	*d*
$X(np \rightarrow (n+1)s); ^1(\pi \rightarrow \pi^*); ^1(\sigma \rightarrow \sigma^*)$	XI	*d*	*d*	>45 000 (1.2)	>45 000 (1.3)	*d*

[a] Entries are in the form $\bar{\nu}_{max}/cm^{-1}$ ($N = I_\parallel/I_\perp$); sh = shoulder. [b] See ref 16. [c] For this compound, bands II and IV are the analogous σ(MoAs) excitations. See ref 1b. [d] Not observed. [e] These values are about 2000 cm^{-1} lower than the true values because of extraneous absorption effects. [f] This polarization ratio was affected by stray light for this weakly emissive compound.

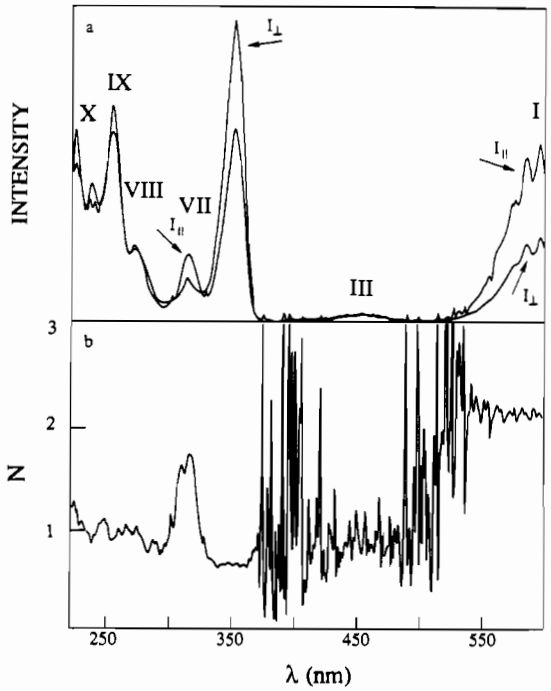

Figure 6. (a) Polarized fluorescence excitation spectra of $Mo_2Br_4(PMe_3)_4$ in 2-methylpentane at 77 K. (b) Wavelength dependence of N for (a).

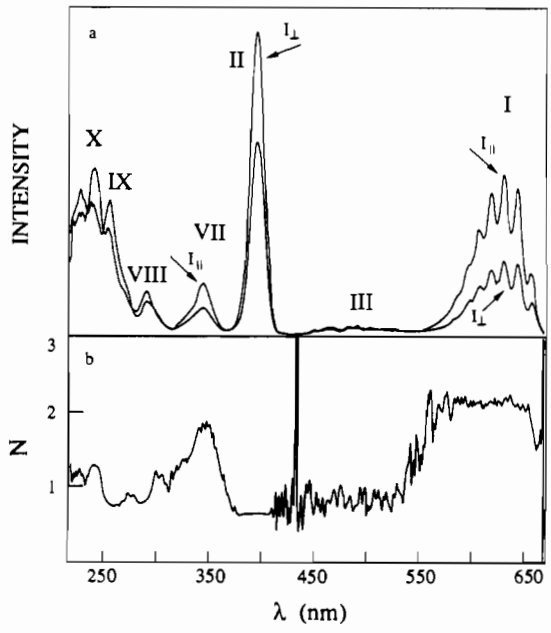

Figure 7. (a) Polarized fluorescence excitation spectra of $Mo_2I_4(PMe_3)_4$ in 2-methylpentane at 77 K. (b) Wavelength dependence of N for (a).

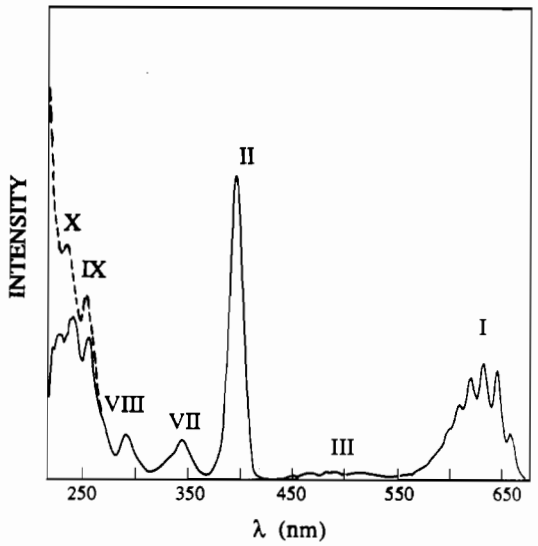

Figure 8. Isotropic-equivalent fluorescence excitation spectra ($I_\parallel + 2I_\perp$) of $Mo_2I_4(PMe_3)_4$ in 2-methylpentane at 77 K: (—) uncorrected for polarizer absorption; (- - -) corrected for polarizer absorption.

The intermediate values of N (N = 0.7–0.9) for band III, the $^1(\pi \rightarrow \delta^*)$ transition, are also explicable: our single-crystal measurements revealed a moderately intense, $\parallel z$-polarized vibronic component in addition to the $\perp z$-polarized dipole-allowed transition.[1a] Such a situation is one explanation for intermediate values of N, but one that is probably only applicable to relatively weak bands such as III. For the intense UV-absorption region, the observed intermediate values of N (Table II) are for the most part indicative of overlapping transitions of different polarization. One manifestation of this is that while bands I–III (which overlap very little) show wavelength-independent values of N across the absorption bands, N varies rather continuously through the UV region, with extremes of N often not coinciding with absorption or excitation band maxima.

For the shortest-wavelength region (λ < 250 nm), the excitation spectra are significantly affected by extraneous absorption. The largest contributor is absorption by the excitation polarizer, which is opaque below 220 nm. Figures 5 and 8 show isotropic-equivalent excitation spectra that have been corrected for polarizer absorption. These spectra have not been corrected for solvent/dewar absorption, which would affect data for λ ≤ 240 nm. For the two $Mo_2Cl_4L_4$ complexes, the effect of the polarizer absorption is simply to reduce short-wavelength intensity in the excitation spectra. The fact that the polarization ratios are roughly wavelength independent through the two intense bands in the deep UV region (Figure 4) indicates that stray-light effects are not important, since the ratio of stray light to real signal must be increasing rapidly near the absorption cutoff at 220 nm. This is not the case for $W_2Cl_4(PMe_3)_4$, however, for which we were unable to eliminate stray-light effects for λ < 250 nm due to the fact that

the compound is only weakly emissive. For $Mo_2Br_4(PMe_3)_4$ and $Mo_2I_4(PMe_3)_4$, the counteracting effects of rapidly increasing real absorption by the compounds and rapidly increasing extraneous absorption by the excitation polarizer combine to produce false peaks near 225 nm (Figures 6 and 7) that can be removed by correction, as shown for $Mo_2I_4(PMe_3)_4$ in Figure 8.

Electronic Transition Assignments. The spectra of $Mo_2Cl_4(PMe_3)_4$ and $Mo_2Cl_4(AsMe_3)_4$ show two intense bands in the UV region (Table I) that are near the energy estimated for $\pi(Cl) \rightarrow \delta^*$ transitions; these bands are labeled IX and X. The polarization ratio of IX indicates that this electronic transition is $\perp z$-dipole allowed, while that of X is slightly higher, suggesting that it consists of overlapping $\perp z$- and $\parallel z$-polarized electronic absorptions. There are two analogous bands each in the spectra of $Mo_2Br_4(PMe_3)_4$ and $Mo_2I_4(PMe_3)_4$, which we have also labeled IX and X. The polarization ratio of band X is somewhat higher for the iodo complex than for the other compounds, which may in part represent underlying intensity due to a higher-energy $\parallel z$-polarized transition (vide infra). The higher energies of the analogous bands of $W_2Cl_4(PMe_3)_4$ are as expected.

In addition to the intense, predominantly $\perp z$-polarized bands II, IX, and X, there are two weaker UV features labeled VII and VIII. The latter of these is also predominantly $\perp z$-polarized, but band VII has considerable $\parallel z$ polarization. The energies of all five bands shift similarly among the compounds we have examined, which strongly suggests that they are all due to LMCT transitions. Indeed, the number of bands observed—four with $\perp z$ polarization and one with $\parallel z$ polarization—is just what is predicted for the dipole-allowed LMCT transitions to δ^*, and the total energetic spread of these bands (ca. 2 eV) is consistent with the calculations (vide supra).[7,10]

There are two complications with this simple picture, however. First, since all of these bands shift with halide, it is not obvious that one can be identified as $e(\sigma(MP)) \rightarrow \delta^*$. Second, consideration of Figure 1 indicates that only the $\pi_\perp(X)$ orbitals are appropriately oriented for good spatial overlap with the metal d_{xy} orbitals that constitute δ^*. Since such interaction is required to yield intensity for charge-transfer transitions, the zero-order prediction is that $e(\pi_\perp(X)) \rightarrow \delta^*$ should be the only intense $\perp z$-polarized LMCT transition; the other two $\perp z$-polarized bands should be relatively weak. The $\parallel z$-polarized $b_1(\pi_\perp(X)) \rightarrow \delta^*$ band should also be weak, since the MMX bond angles are 110–112°, and hence the z-axis projections of the M–X bond dipole moments are small (the intensity would be zero for ∠MMX = 90°).

The contrary observation of three intense $\perp z$-polarized LMCT transitions demands that mixing must occur among the various ligand orbitals, thus yielding mixing of the various LMCT transitions. We proposed[1b] such an explanation to account for the halide sensitivity of band II, and the various theoretical calculations[7,10] do indicate considerable mixing among the ligand levels.

Inspection of Figure 1 indicates how mixing can occur between the e-symmetry $\pi_\perp(X)$ and $\sigma(P)$ orbitals, since there will be overlap on each metal center that will be enhanced as the spatial extent of the ligand orbitals increases. While $\pi_\perp(X)$ does not appear to have significant direct overlap with $\sigma(X)$, indirect mixing of $\pi_\perp(X)$ and $\sigma(X)$ is possible because of the overlap of $\sigma(X)$ and $\sigma(P)$ across the metal–metal bond; this is illustrated in the following diagram:

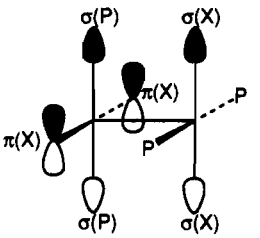

We propose that these three mixed orbitals lead to the three intense, $\perp z$-polarized LMCT transitions. On the other hand, there is no obvious way to mix $\pi_\parallel(X)$. We therefore assign the weak band VIII to the $e(\pi_\parallel(X)) \rightarrow \delta^*$ transition, band VII being the $\parallel z$-polarized $b_1(\pi_\perp(X)) \rightarrow \delta^*$ transition.

We next consider whether any reasonable case can be made for assigning dominant configurations for bands II, IX, and X. For the chloro complexes of this study, band II is at much lower energy than bands IX and X, and is considerably weaker than them. For this and other reasons previously discussed,[1a,b] it seems reasonable to assign this band to the $^1(e(\sigma(MP)) \rightarrow \delta^*)$ transition. The intensities of bands IX and X are similar to each other, so the $e(\pi_\perp(X))$ and $e(\sigma(MX))$ levels are inferred to be strongly mixed.

As the halide becomes more reducing, mixing with $e(\sigma(MP))$ should increase; it should then decrease again as halide levels move above $\sigma(MP)$ levels. This is an example of an avoided crossing. For $Mo_2I_4(PMe_3)_4$, band II now appears to be the *most* intense of the LMCT bands (Figure 8), which suggests that crossing has occurred. Indeed, there is an independent reason to conclude that the iodo complex is probably past the crossing point, that is, that band II is better described as $\pi_\perp(I) \rightarrow \delta^*$. Cotton and Poli[14] have recently reported electronic spectra for compounds of the type $Mo_2I_4(RCN)_4$. The EtCN complex shows an intense band at 27 800 cm^{-1}, which evidently must be assigned to a $^1(\pi(I) \rightarrow \delta^*)$ transition, since nitriles are extremely poorly reducing.[15,16]

An additional complication is that the shapes of bands VII and VIII indicate that there are weak underlying absorption bands. We believe this is because triplet LMCT states, which can reasonably be expected to lie a few thousand wavenumbers below the singlet states,[1a,11] are also present in this region. These nominally spin-forbidden transitions are expected to intensify as the mass of either the ligands or the metal increases, due to spin–orbit coupling considerations, and this appears to be consistent with our data for bands VII and VIII, particularly for $W_2Cl_4(PMe_3)_4$. The observation of high-intensity singlet–triplet LMCT transitions for this compound is consistent with the fact that band IV ($^3(\sigma(WP) \rightarrow \delta^*)$) is also fairly intense, whereas it is so weak for the other compounds that it can only be discerned in low-temperature single-crystal spectra.[1a] Indeed, it is noteworthy that band VII of the tungsten compound does not show pronounced $\parallel z$ polarization, in contrast to those of the molybdenum compounds; it may be dominated by singlet–triplet transitions.

We finally consider the intense absorption (band XI) whose maximum lies at greater than 50 000 cm^{-1} for $Mo_2Br_4(PMe_3)_4$ and $Mo_2I_4(PMe_3)_4$. A likely assignment is to halide-localized $np \rightarrow (n+1)s$ transitions, which occur in this vicinity for free halide ions.[17] One favorable aspect of this assignment is that it is consistent with the decreased fluorescence efficiency seen for excitation into these bands (Figures 2 and 3); the halide-localized excited states might communicate poorly with the lower-energy metal–metal excited states. However, the fact that excitation into the rising edge of band XI yields polarization ratios greater than 1 (Table II) leads us to suspect that band XI might also consist, at least in part, of the $\parallel z$-polarized $^1(\pi \rightarrow \pi^*)$ transition. We have certainly not identified any plausible lower-energy candidates (assuming that $^1(\pi \rightarrow \pi^*)$ is an intense transition), so if nothing else, the energy of band XI provides a lower limit for that of $^1(\pi \rightarrow \pi^*)$.

Summary and Comparisons to Related Systems. We have made self-consistent assignments for the UV absorption spectra of several $M_2X_4L_4$ compounds, despite their complexity. With the exception of the poorly characterized band XI, all of the absorption bands can be attributed to LMCT excitations into the δ^* orbital. It has

(14) Cotton, F. A.; Poli, R. *J. Am. Chem. Soc.* **1988**, *110*, 830–841.
(15) The $Mo_2I_4(RCN)_4$ complexes are unstable with respect to elimination of nitrile,[14] so only semiquantitative spectra could be measured. Of the spectra reported in ref 14, we choose to compare our data to their spectrum of the EtCN complex, because the relative intensities of bands I–III in this spectrum appear similar to those found by us[1b] for $Mo_2I_4(PMe_3)_4$.
(16) We will retain, for brevity, the general designation of $\pi(X) \rightarrow \delta^*$, $\sigma(MP) \rightarrow \delta^*$, etc., although these are only zero-order descriptions in all cases, and may be incorrect for the iodo complex.
(17) (a) Jorgensen, C. K. *Adv. Chem. Phys.* **1963**, *5*, 33–146. (b) Fox, M. F. In *Concepts of Inorganic Photochemistry*; Adamson, A. W., Fleischauer, P. D., Eds.; Wiley: New York, 1975; Chapter 8.

proven neither necessary nor desirable to assign these features to excitations into higher energy virtual orbitals (such as π^*). Thus, excitations of the latter type must either be considerably weaker than the assigned LMCT excitations (as we believe to be true for excitations such as $^1(\delta \rightarrow \pi^*)$) or must lie to still higher energy.

It is of interest to compare our assigned spectra to those of related compounds. As previously noted,[1a] it is possible to place a lower limit of 30 000 cm^{-1} on the energies of allowed LMCT states for $Mo_2Cl_8^{4-}$, and this is particularly consistent with our assignment of $^1(\sigma(MP) \rightarrow \delta^*)$ for $Mo_2Cl_4(PMe_3)_4$. A weak ($\epsilon \sim 200$) feature observed by Fanwick et al.[18] at 28 985 cm^{-1} in the single-crystal spectrum of $K_4[Mo_2Cl_8]\cdot 2H_2O$ has been assigned to $^3(\pi(Cl) \rightarrow \delta^*)$,[1a] and our present results suggest that it is still the most reasonable assignment.

Detailed assignments have previously been presented for the $Re_2Cl_8^{2-}$ and $Re_2Br_8^{2-}$ ions.[19,20] There are close similarities to our present results in that two intense $\perp z$-polarized LMCT bands are observed (together with a cluster of spin-forbidden LMCT transitions ca. 4000 cm^{-1} to lower energy[19,20]), as well as an intense $\|z$-polarized transition assigned to $^1(\pi \rightarrow \pi^*)$ at ca. 40 000 cm^{-1}. It is not clear why $^1(\pi \rightarrow \pi^*)$ should lie at much lower energy for the Re(III) halides than for the Mo(II) and W(II) compounds. Since the LMCT transitions of the $Re_2X_8^{2-}$ compounds should include a $\|z$-polarized $^1(\pi(X) \rightarrow \delta^*)$ excitation (the spin- and dipole-allowed $\pi(X) \rightarrow \delta^*$ transitions of $M_2X_8^{n-}$ include one $\|z$- and two $\perp z$-polarized transitions), further studies of these and related ions, such as $Re_2F_8^{2-}$ (for which LMCT transitions should be very strongly blue-shifted), are desirable.

Relevance to Photochemistry and Photophysics. The $Mo_2Cl_4(PR_3)_4$ complexes undergo photolysis in halocarbon solution upon 254-nm irradiation to yield halide-bridged binuclear Mo(III) complexes as products.[3] Quantum yields at 254 nm were reported to be 5–6%, while no photochemistry was observed for visible or near-UV irradiation. The photoreaction was suggested to proceed via LMCT excited states, and our present work confirms that absorption bands near 254 nm are indeed due to LMCT transitions.

Our emission excitation spectra in halocarbon solvents are not inconsistent with the claimed yields, since we do not believe that our various corrections can be applied accurately enough to detect emission losses as small as 5%, particularly near the solvent absorption limit. However, our results definitely exclude the possibility that the photochemistry emanates from a photochemical transient (such as a radical pair) that is formed in high yield from the LMCT states but that largely reverts to ground-state starting material.

A second comparison of interest is to the transient-absorption studies of Winkler et al.[21] These workers reported that $Mo_2Cl_4(PBu^n_3)_4$ exhibits, in a variety of solvents, not only the emissive $^1(\delta\delta^*)$ transient but also a second, nonemissive transient that decays to the ground state on a longer time scale than $^1(\delta^* \rightarrow \delta)$. As judged by the magnitude of long-lived transient bleaching, the yield of the second transient is 30–40%.

One aspect that was not completely established in Winkler's study[21] was whether the second transient was formed via a nonradiative decay process from the thermally equilibrated $^1(\delta\delta^*)$ excited state or whether the two transients were both formed during decay of the initially prepared excited states. Our present results, together with a previous study[12] of the excitation spectrum of $Mo_2Cl_4(PBu^n_3)_4$, strongly support the first possibility, since the observed wavelength independence of the $^1(\delta^* \rightarrow \delta)$ fluorescence quantum yield (hence, $^1(\delta\delta^*)$ formation yield) would imply, implausibly, a complete wavelength independence of the branching ratio for formation of two competitive transients. We furthermore note that the second transient is evidently formed via a previously characterized[1d,f] thermally activated nonradiative process, since this is overwhelmingly the dominant decay process of the $^1(\delta\delta^*)$ excited state of $Mo_2Cl_4(PBu^n_3)_4$ at room temperature.[22] The identity of the long-lived transient remains unclear, but the outstanding possibility at this point is the low-lying $^3(\delta\delta^*)$ state.[4] Winkler et al.[21] considered another possibility, namely the $^3(\pi\delta^*)$ excited state. However, they noted several difficulties with this assignment, to which we now add that slow interconversion of the closely spaced $^3(\pi\delta^*)$ and $^1(\delta\delta^*)$ excited states (required by the transient kinetics) seems very unlikely in view of the rapid and efficient decay of the wide variety of upper excited states (including $^1(\pi\delta^*)$ to $^1(\delta\delta^*)$) that is required by our present results. There is a possible role for the $^3(\pi\delta^*)$ state, however. This state can be reasonably expected to lie to slightly higher energy of $^1(\delta\delta^*)$, given the experimental[1a] location of the $^1(\pi \rightarrow \delta^*)$ transition, and a triplet state should show decay rates to the $^3(\delta\delta^*)$ excited state that are enhanced relative to those of singlet states such as $^1(\delta\delta^*)$; thus, this state might provide the thermally activated nonradiative decay pathway.

Acknowledgment. We thank Bill Schneider and Bruce Bursten for several helpful discussions and for providing us the results of their calculations prior to publication. This research was supported by National Science Foundation Grants CHE89-22067 (H.B.G.) and CHE86-57422 (M.D.H.).

Registry No. $Mo_2Cl_4(PMe_3)_4$, 67619-17-4; $Mo_2Cl_4(AsMe_3)_4$, 105064-90-2; $Mo_2Br_4(PMe_3)_4$, 89707-70-0; $Mo_2I_4(PMe_3)_4$, 89637-15-0; $W_2Cl_4(PMe_3)_4$, 73495-54-2.

(18) Fanwick, P. E.; Martin, D. S.; Cotton, F. A.; Webb, T. R. *Inorg. Chem.* **1977**, *16*, 2103–2106.
(19) (a) Mortola, A. P.; Moskowitz, J. W.; Rösch, N.; Cowman, C. D.; Gray, H. B. *Chem. Phys. Lett.* **1975**, *32*, 283–286. (b) Cowman, C. D.; Trogler, W. C.; Gray, H. B. *Isr. J. Chem.* **1977**, *15*, 308–310. (c) Cowman, C. D. Ph.D. Thesis, California Institute of Technology, 1974.
(20) (a) Trogler, W. C.; Cowman, C. D.; Gray, H. B.; Cotton, F. A. *J. Am. Chem. Soc.* **1977**, *99*, 2993–2996. (b) Miskowski, V. M. Unpublished data.
(21) Winkler, J. R.; Nocera, D. G.; Netzel, T. L. *J. Am. Chem. Soc.* **1986**, *108*, 4451–4458.
(22) At room temperature, the thermally activated nonradiative process does not contribute significantly to the decay of the $^1(\delta\delta^*)$ state of $Mo_2Cl_4(PMe_3)_4$,[1d,f] and Winkler has recently found (private communication) that the second transient is not observed for this compound (the transient and emission-decay kinetics are identical). Our interpretation is consistent with these facts.